Kinematic model of 1 DoF elbow joint with a pair of agonist-antagonist muscles

Python code can be found here:

https://github.com/anagamori/1dof_elbow_model.git

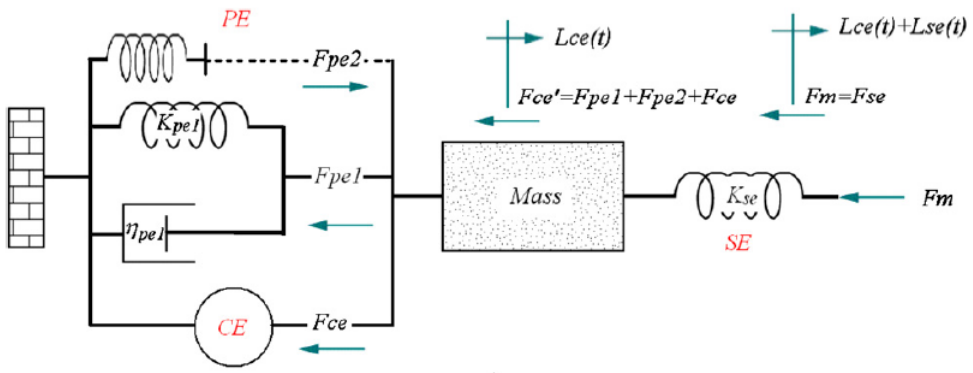

Figure 1: The mechanical structure of a muscle model without pennation angle.

Muscle Model

This model of a musculotendon unit (muscle + tendon + aponeurosis) consists of five elements: a mass, a contractile element, two passive elements and a series elastic element (Fig. 1) (Cheng et al., 2000; Song, Raphael, et al., 2008; Tsianos et al., 2012). The mass, M_m, presents that of a musculotendon unit. The contractile element generates muscle force, F_{ce}, arising from contractions of muscles fibers. This muscle force represents summed forces from individual motor unit forces, each of which contains a single motoneuron and a number of muscle fibers that the motoneuron innervates. The two passive elements, F_{pe1} and F_{pe2}, simulate parallel elasticity of muscle fascicles. The muscle contraction causes a change in the length of a series-elastic element. This length change in the series-elastic element generates force on a skeletal system through its attachment site (i.e. insertion) and cause joint rotation. All model parameters except for those specific to our model are given in Table 1 of Tsianos et al. (2012).

Contractile Element

The contractile element represents the force generating mechanisms of muscles (i.e. motoneurons and muscle fibers that they innervate), which converts the neural activation signal, U, into muscle force F_{ce}. The neural activation signal is a simplified representation of overall synaptic input that the entire motor unit population receives and the value is normalized between 0 and 1. For the version of the model presented here, a muscle consists of two groups of motor units: slow and fast.

In this model, U is first converted into the effective neural activation, U_{eff}, to account for the

first-order dynamics due to calcium kinetics using the following equation:

$$\dot{U}_{eff} = \frac{U - U_{eff}}{T_U} \tag{1}$$

$$T_U = \begin{cases} T_{rise} exp[-(U - U_{eff}) \cdot ln(T_{rise} * 1000)], U \geq U_{eff} \\ T_{fall}, U < U_{eff} \end{cases}$$

where

$$T_{rise} = 0.38 U_{th}^{fast^2} + 0.8 U_{th}^{fast} + 0.14$$

$$T_{fall} = -0.32 U_{th}^{fast^4} + 0.82 U_{th}^{fast^3} - 0.28 U_{th}^{fast^2} + 0.014 U_{th}^{fast} + 0.09.$$

U_{th}^{fast} denotes the recruitment threshold of the fast motor unit defined below.

The effective neural activation, U_{eff}, recruits the motor units based on the recruitment profiles of the fiber type (i.e. slow or fast). The 'firing frequency' of each motor unit, f_{env}^i linearly increases from its minimum (f_{min}^i) to its maximum (f_{max}^i) with an increase in the value of U_{eff}, where i denotes the individual motor unit type. To simulate the rise and fall time of calcium dynamics, the firing frequency of the motor unit is passed through two separate first-order dynamics using the following equation:

$$f_{int}^i = \frac{f_{env}^i - f_{int}^i}{T_f^i} \tag{2}$$

$$f_{eff}^i = \frac{f_{int}^i - f_{eff}^i}{T_f^i} \tag{3}$$

$$T_f = \begin{cases} T_{f1} \bar{L}_{ce}^2 + T_{f2} f_{env}^i(t), \dot{f}_{eff}^i \geq 0 \\ (T_{f3} + T_{f4} A f^i)/\bar{L}_{ce}, \dot{f}_{eff}^i < 0 \end{cases}$$

The activation level of motor units, Af^i, (i.e. the number of cross-bridges in the force-generating state) as a function of their firing frequency (f_{eff}^i) follows a sigmoidal relationship Brown et al.,

1999. Furthermore, the activation-frequency relationship depends also on the length and velocity of muscle and activation history Brown et al., 1999. To simulate these effects, the activation-frequency relationship of the motor units is expressed as follows:

$$Af^i = \begin{cases} 1 - exp\left[-\left(\frac{Yf^i_{eff}}{a_f n_f}\right)^{n^i_f}\right], slow \\ 1 - exp\left[-\left(\frac{S^i f^i_{eff}}{a_f n_f}\right)^{n^i_f}\right], fast \end{cases} \tag{4}$$
$$n^i_f = n_{f0} + n_{f1}\left(\frac{1}{\bar{L}_{ce}} - 1\right)$$

where Y and S are the sag and yielding properties of slow and fast motor units. Those properties are implemented using the following equations:

$$\dot{S_i}^i(t) = \frac{a_S - S^i_i(t)}{T_S},$$
$$a_S = \begin{cases} a_{S1}, f^i_{eff}(t) < 0.1 \\ a_{S2}, f^i_{eff}(t) \geq 0.1 \end{cases} \tag{5}$$

$$\dot{Y_i}(t) = \frac{1 - c_Y[1 - exp(-\frac{|V_{ce}|}{V_Y})] - Y(t)}{T_Y}. \tag{6}$$

The length-dependence of muscle force, known as the force-length relationship, arises from the interaction between the muscle length and the number of cross-bridges that can be formed (Tsianos & Loeb, 2017). This relationship is captured by scaling muscle force by FL^i, which can be described as follows:

$$FL^i = exp(-\left|\frac{L^\beta_{ce} - 1}{\omega}\right|^\rho), \tag{7}$$

where the parameters, ω, β and ρ are fiber-type specific.

Active muscle force is known to depend on the speed at which muscle contracts (Tsianos & Loeb, 2017). Compared to an isometric condition (muscle length = constant), muscle force decreases

when the muscle is shortening while it increases when the muscle is lengthening. This force-velocity relationship can be described as follows:

$$FV^i = \begin{cases} (V_{max} - V_{ce}/[V_{max} + (c_{v0} + c_{v1} * L_{ce})V_{ce}]), V_{ce} \leq 0 \\ [b_v - (a_{v0} + a_{v1}L_{ce} + a_{v2}L_{ce}^2)V_{ce}]/(b_v + V_{ce}), V_{ce} < 0 \end{cases} . \quad (8)$$

The values of the coefficients in the above equations depend on fiber types as in the force-length relationship (Song, Lan, et al., 2008; Tsianos et al., 2012).

The normalized active force from the contractile element is then computed as follows:

$$F_{ce} = \sum_{i=1}^{n} rF_{pcsa}^i \cdot W^i \cdot Af^i \cdot (FL^i \cdot FV^i + F_{pe2}). \quad (9)$$

F_{pe2} is passive, resistive force against shortening (see its description below). rF_{pcsa}^i is defined as follows:

$$rF_{pcsa}^i = \begin{cases} 0, U \leq U_{th}^i \\ \frac{F_{pcsa}^i}{1-U_{th}^i}(U - U_{th}^i), U > U_{th}^i \end{cases} \quad (10)$$

where U_{th}^i defines the recruitment threshold of slow and fast motor units, which are set to 0.001 and 0.4, respectively. W^i is computed based on the threshold of each motor unit type, U_{th}^i, and the effective activation as follows:

$$W^i = \frac{U_{eff} - U_{th}^i}{\sum_{k=1}^{i}(U_{eff} - U_{th}^k)} \quad (11)$$

Passive Elements

The model includes two passive elements in parallel to the contractile element: passive element 1 and 2 generating force against muscle stretch (F_{pe1}) and against shortening (F_{pe2}), respectively.

The force generated by passive element 1 can be described as follows:

$$\overline{F}_{pe1}(L_{ce}, V_{ce}) = c_1 k_1 ln\left[exp\left(\frac{L_{ce}/L_{ce}^{max} - L_{r1}}{k_1}\right) + 1\right] + \eta V_{ce}. \tag{12}$$

The force generated by passive element can be described as follows:

$$\overline{F}_{pe2}(L_{ce}) = c_2\{exp[k_2(L_{ce} - L_{r2})] - 1\}. \tag{13}$$

Series-Elastic Element

The force generated by a series-elastic element is described as follows:

$$\overline{F}_{se}(L_{se}) = c^T k^T ln\left[exp\left(\frac{L_{se} - L_r^T}{k_T}\right) + 1\right]. \tag{14}$$

Contractile Dynamics

At an equilibrium, force generated by the muscle and tendon become equal (Fig. 1). Any deviation from this equilibrium due to changes in neural activation to the muscle or those inherent in the motor unit force generation mechanisms (i.e. unfused tetanic contractions) causes changes in the length of muscle and a series-elastic element (i.e. tendon + aponeurosis). This contraction dynamics between muscle and the series-elastic element can be described as follows (He et al., 1991):

$$\begin{aligned} A_{ce}(t) \cdot L_{ce0}(t) =& \frac{1}{M_m}[F_0 \cdot \bar{F}_{se}(t) \cdot cos\alpha - (F_{ce}(t) + F_0 \cdot \bar{F}_{pe1}(t)) \cdot cos^2\alpha] \\ &+ \frac{(V_{ce}(t) \cdot L_{ce0})^2 \cdot tan^2\alpha}{L_{ce}(t) \cdot L_{ce0}}, \end{aligned} \tag{15}$$

with an constraint given by the following equation:

$$L_{mt}(t) = L_{ce}(t) \cdot L_{ce0} \cdot cos\alpha + L_{se}(t) \cdot L_{se0}, \tag{16}$$

where α, L_{ce}, V_{ce}, A_{ce}, L_{se} and L_{mt} are pennation angle (angle between muscle's line of action and that of a series-elastic element), muscle length normalized to optimal muscle length, normalized

Table 1: **Model parameters for muscle based on architectural parameters of *biceps long head*** (Song, Lan, et al., 2008)

Maximum muscle force, F_0 (N)	434
Optimal muscle length, L_{ce0} (cm)	21.5
Optimal tendon length, L_{se0} (cm)	16.3
Pennation angle, α (deg)	0

muscle velocity, normalized muscle acceleration, series-elastic element length normalized to its optimal length and musculotendon unit length in cm. F_0 determines maximum tetanic force of muscle as described below. The resulting muscle acceleration is then integrated to update the muscle length, which is used to compute the series-elastic element length from the relationship described in Eq. 16.

Muscle Mass

The relationship between the maximum force that muscle can generate (F_0) and its mass is described as follows (Lieber et al., 1990):

$$F_0 = \frac{M_m \cdot cos(\alpha) \cdot \epsilon}{\rho \cdot L_{ce0}}, \tag{17}$$

where M_m, ρ, ϵ and L_{ce0} are muscle mass, muscle density (1.06 g/cm$_3$), specific tension (31.8 N/cm$_2$) and optimal fascicle length, respectively. From this relationship, M_m is derived for a user-specified value of F_0.

One degree-of-freedom elbow joint

A schematic representation of a model of a 1 degree-of-freedom elbow joint is shown in Fig. 2. The model consists of two identical limb segments modeled as a cylindrical rod. The length and diameter of the segment are set to 45 cm and 5 cm, respectively. The mass, M, equals to 100 g. The proximal segment is attached to the ground, permitting no rotation. The distal segment

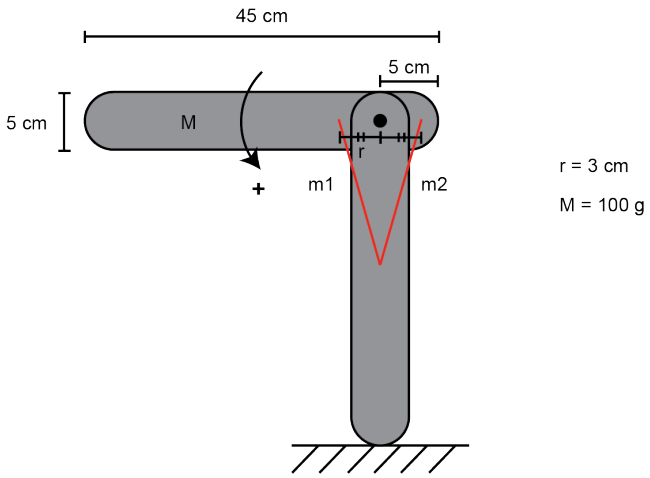

Figure 2: A schematic representation of a 1 DoF elbow joint.

rotates around an axis placed 5 cm inside of its one end. The counter-clockwise rotation (or elbow flexion) is defined as a position angle.

The joint rotation is controlled by two identical muscles defined above. The movement arm, r, of both muscles are also set identical to 3 cm but with opposite signs. The joint kinematics introduced by the activation of those muscles follows the Newton's second law such that

$$\ddot{\theta} = \frac{1}{I}(\tau_1 + \tau_2 - b \cdot \dot{\theta} - k \cdot \theta), \tag{18}$$

where τ_1 and τ_2 are torque generated by muscle 1 and 2, respectively, θ is the joint angle in radian and I is the inertia of the distal limb rotating around the axis defined in Fig. 2. b and k define the external viscosity and stiffness, both of which are set to 0. The resulting joint rotation causes changes in the musculotendon length (i.e. L_{mt}) of muscles, which are computed as follows:

$$\Delta L^i_{mt} = r^i \cdot \Delta\theta, \tag{19}$$

where the superscript, i, denotes muscle. This equation is used to update the musculotendon length in Eq. 16 every time step.

References

Brown, I. E., Cheng, E. J., & Loeb, G. E. (1999). Measured and modeled properties of mammalian skeletal muscle. II. The effects of stimulus frequency on force-length and force-velocity relationships. *Journal of Muscle Research and Cell Motility*, 17.

Cheng, E. J., Brown, I. E., & Loeb, G. E. (2000). Virtual muscle: A computational approach to understanding the effects of muscle properties on motor control. *Journal of Neuroscience Methods*, *101*(2), 117–130. https://doi.org/10.1016/S0165-0270(00)00258-2

He, J., Levine, W. L., & Loeb, G. E. (1991). Feedback Gains for Correcting Small Perturbations to Standing Posture. *IEEE Transactions on automatic control*.

Lieber, R. L., Fazeli, B. M., & Botte, M. J. (1990). Architecture of selected wrist flexor and extensor muscles. *The Journal of Hand Surgery*, *15*(2), 244–250. https://doi.org/10.1016/0363-5023(90)90103-X

Song, D., Lan, N., Loeb, G. E., & Gordon, J. (2008). Model-Based Sensorimotor Integration for Multi-Joint Control: Development of a Virtual Arm Model. *Annals of Biomedical Engineering*, *36*(6), 1033–1048. https://doi.org/10.1007/s10439-008-9461-8

Song, D., Raphael, G., Lan, N., & Loeb, G. E. (2008). Computationally efficient models of neuromuscular recruitment and mechanics. *Journal of Neural Engineering*, *5*(2), 008. https://doi.org/10.1088/1741-2560/5/2/008

Tsianos, G. A., Rustin, C., & Loeb, G. E. (2012). Mammalian Muscle Model for Predicting Force and Energetics During Physiological Behaviors. *IEEE Transactions on Neural Systems and Rehabilitation Engineering*, *20*(2), 117–133. https://doi.org/10.1109/TNSRE.2011.2162851

Tsianos, G. A., & Loeb, G. E. (2017). Muscle and Limb Mechanics (R. Terjung, Ed.). In R. Terjung (Ed.), *Comprehensive Physiology*. Hoboken, NJ, USA, John Wiley & Sons, Inc. https://doi.org/10.1002/cphy.c160009